

# SkyMapper and EMP stars

**Mike Bessell**  
on behalf of  
**the EMP team**



Australian  
National  
University

*Research School of Astronomy and Astrophysics*

CAASTRO 2014



# The discovery of the ancient star with no Fe lines.

SkyMapper  
2.3m WiFeS  
Magellan MIKE

S. C. Keller, M. S. Bessell, A. Frebel\*, A. R. Casey, M. Asplund□, H. R. Jacobson\*, K. Lind, J. E. Norris, D. Yong, A. Heger□, Z. Magic, G. S. Da Costa, B. P. Schmidt, & P. Tisserand



## A single low-energy, iron-poor supernova as the source of metals in the star SMSS J031300.36–670839.3

S. C. Keller<sup>1</sup>, M. S. Bessell<sup>1</sup>, A. Frebel<sup>2</sup>, A. R. Casey<sup>3</sup>, M. Asplund<sup>4</sup>, H. R. Jacobson<sup>2</sup>, K. Lind<sup>5</sup>, J. E. Norris<sup>6</sup>, D. Yong<sup>7</sup>, A. Heger<sup>8</sup>, Z. Magic<sup>1,5</sup>, G. S. Da Costa<sup>1</sup>, B. P. Schmidt<sup>1</sup> & P. Tisserand<sup>1</sup>

The element abundance ratios of four low-mass stars with extremely low metallicities (abundances of elements heavier than helium) indicate that the gas out of which the stars formed was enriched in each case by at most a few—and potentially only one—low-energy supernova<sup>9,10</sup>. Such supernovae yield large quantities of light elements such as carbon but very little iron. The dominance of low-energy supernovae seems surprising, because it had been expected that the first stars were extremely massive, and that they disintegrated in pair-instability explosions that would rapidly enrich galaxies in iron<sup>11</sup>. What has remained unclear is the yield of iron from the first supernovae, because hitherto no star has been unambiguously interpreted as encapsulating the yield of a single supernova. Here we report the optical spectrum of SMSS J031300.36–670839.3, which shows no evidence of iron (with an upper limit of  $10^{-7.1}$  times solar abundance). Based on a comparison of its abundance pattern with those of models, we conclude that the star was seeded with material from a single supernova with an original mass about 60 times that of the Sun (and that the supernova left behind a black hole). Taken together with the four previously mentioned low-metallicity stars, we conclude that low-energy supernovae were common in the early Universe, and that such supernovae yielded light-element enrichment with insignificant iron. Reduced stellar feedback both chemically and mechanically from low-energy supernovae would have enabled first-generation stars to form over an extended period. We speculate that such stars may perhaps have had an important role in the epoch of cosmic reionization and the chemical evolution of early galaxies.

Whereas the solar spectrum contains many thousands of spectral lines due to iron and other elements, the high-resolution ( $R = 28,000$ ) optical spectrum of SMSS J031300.36–670839.3 (hereafter SMSS 0313–6708) is remarkable for the complete absence of detectable iron lines. Figure 1 shows a portion of the spectrum that possesses a signal-to-noise ratio ( $S/N$ ) of 100 per resolution element in the vicinity of one of the strongest iron lines (Fe I at 385.9 nm wavelength). The non-detection of iron lines places an upper limit on the iron abundance of the star,  $[Fe/H] < -7.1$ , at a 3 $\sigma$  confidence level. (Here  $[A/B] = \log_{10}(N_A/N_B)_{\text{star}} - \log_{10}(N_A/N_B)_{\odot}$ , where  $N_A/N_B$  is the number ratio of atoms of elements A and B, and the subscript  $\odot$  refers to the solar value.) This upper limit is 30 times lower than the iron abundance in HE 1327–2326, which has  $[Fe/H] = -5.6$  (ref. 2), and is the most iron-deficient star previously known.

The paucity of absorption lines in the spectrum of SMSS 0313–6708 allows us to derive the abundance of only four chemical elements. The calcium abundance is determined to be  $[Ca/H] = -7.0$ . Given that existing studies have shown that  $[Ca/Fe] = +0.4$  for the majority of extremely metal-poor stars<sup>2</sup>, the  $[Ca/H]$  value that we determine would be consistent with an extraordinary low iron abundance limit. We suggest below, however, that the Ca abundance in SMSS 0313–6708

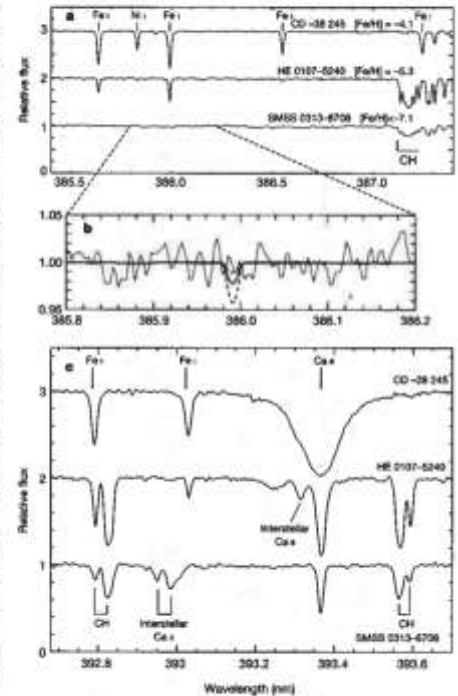


**Figure 1** | A comparison of the spectrum of SMSS 0313–6708 to that of other extremely metal-poor stars. **a–c**, Metal-poor stars of similar temperature and surface gravity are chosen from the literature. The spectrum of SMSS 0313–6708 shows an absence of detectable Fe I lines (**a**) and is dominated by molecular features of CH (**c**). Panel **b** shows the vicinity of what should be one of the strongest iron lines in the ultraviolet/optical wavelength region. Overlaid are synthesized line profiles (1D LTE) for  $[Fe/H] = -7.5$  (dotted line),  $-7.2$  (solid line) and  $-6.9$  (long dashed line).

<sup>1</sup>Research School of Astronomy and Astrophysics, Mount Stromlo Observatory, Cotter Road, Weston, Australian Capital Territory 2611, Australia. <sup>2</sup>Department of Physics, Massachusetts Institute of Technology and Kavli Institute for Astrophysics and Space Research, Cambridge, Massachusetts 02139, USA. <sup>3</sup>Institute of Astronomy, University of Cambridge, Madingley Road, Cambridge CB3 0HA, UK. <sup>4</sup>School of Mathematical Sciences, Monash University, Victoria 3800, Australia. <sup>5</sup>Max-Planck-Institut für Astrophysik, Karl-Schwarzschild-Strasse 1, Garching 85741, Germany.





# SkyMapper

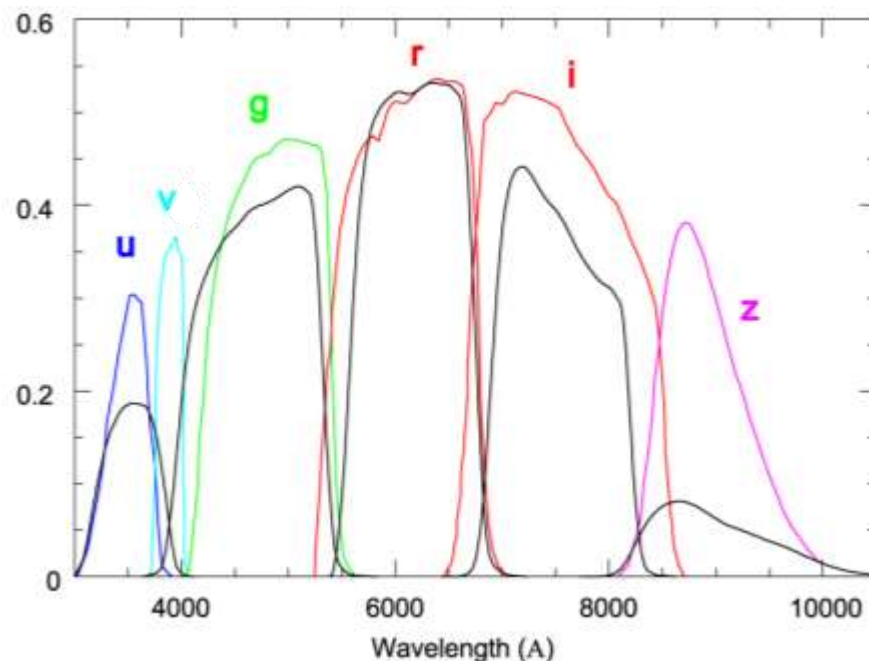
## Optimised for Stellar Astrophysics

We chose to base the SkyMapper passbands on those of the successful SDSS survey. But in 2006 large dielectric filters with uniform transmission could not be made at a price that we could afford, so we decided to look for a colored glass solution. In addition, we realized that we could improve the sensitivity of the UV and blue bands to stellar parameters by tweaking them and including an additional band *v* band.

To do this we separated the red edge of the *u* band and the blue edge of the *g* band putting more of *u* below the Balmer Jump and lowering the metal sensitivity of the *g* band.

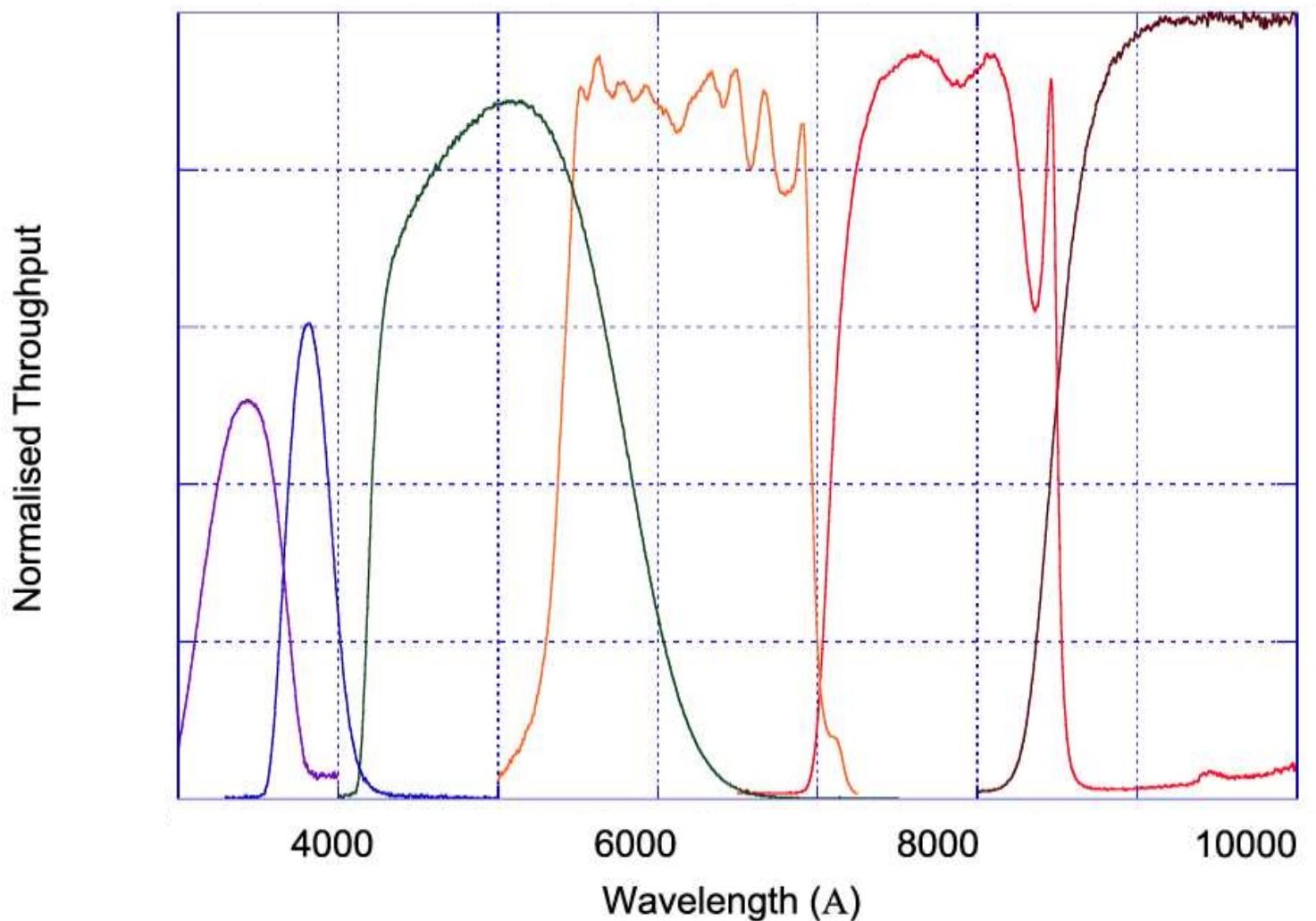
We inserted a narrower *v* band over the region of the strongest metal lines increasing its discrimination at low metallicity.

We thus improved our ability to determine the three important stellar parameters ( $T$ ,  $\log(g)$ ,  $Z$ )

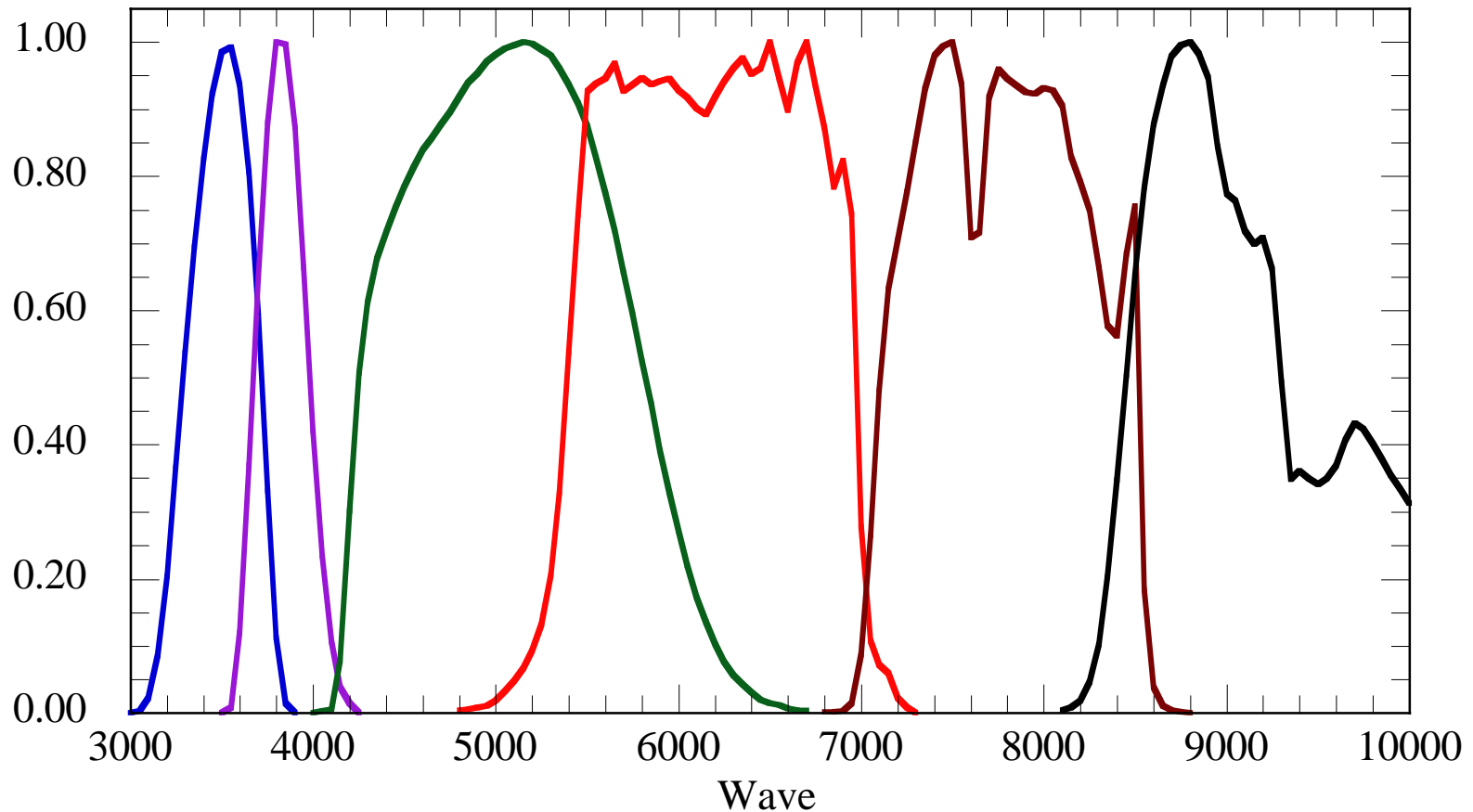




# SkyMapper Filter Set

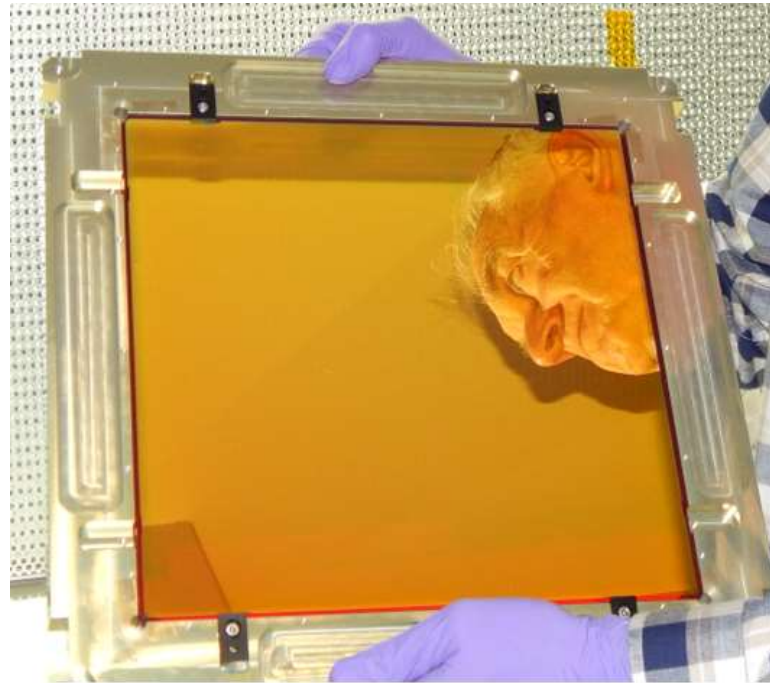
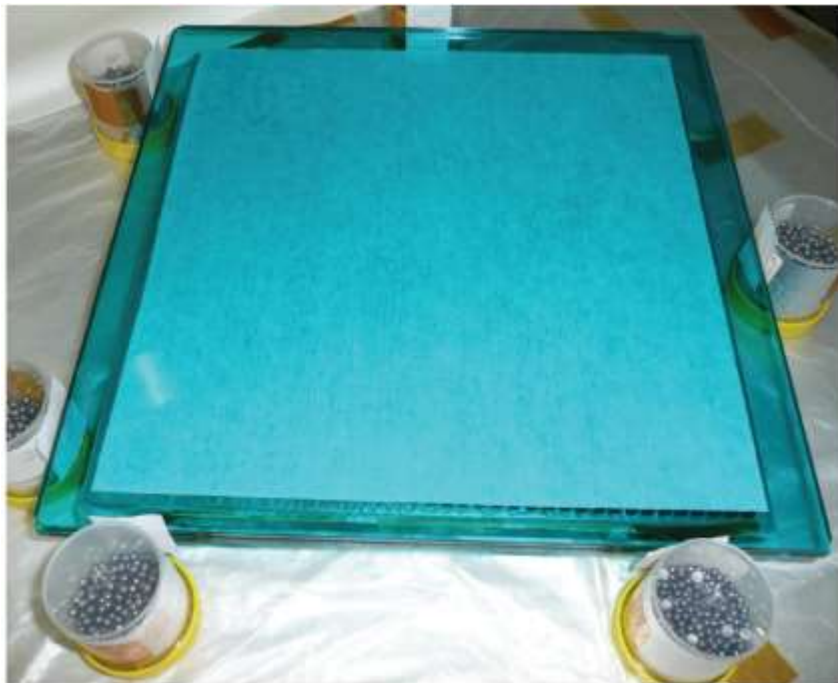


# SkyMapper Passbands ?





# SkyMapper filters



SkyMapper filters are large 310 x 310 x 15 mm. Left, our 3 layer all-glass filter. Right, H $\alpha$  filter coated on a single red glass substrate. In 2006 uniform interference filters could not be made that large. In 2014 Materion can now make them.





# Fundamental SkyMapper standards

We initiated a DTT STIS application with Ralph Bohlin and others to obtain better than 1% spectro-photometry (250nm - 1020nm) for 14 stars, 6 northern, 8 southern, with precise Hipparcos Hp magnitudes (0.002mag). These stars observed from space have no RA, Dec, seasonal effects that can effect ground based systems. We will use the southern and equatorial stars as fundamental standards for SkyMapper. Bohlin's primary DA white dwarf HST standards can also be observed.

| Target    | RA         | Dec (J2000) | V     | Hp    | vrad | Te    | logg       | [Fe/H] | B-V   |
|-----------|------------|-------------|-------|-------|------|-------|------------|--------|-------|
| HD009051  | 01 28 46.4 | -24 20 25.3 | 8.93  | 9.079 | -73  | 4841  | 1.97       | -1.80  | 0.82  |
| HD031128  | 04 52 09.9 | -27 03 50.9 | 9.13  | 9.243 | 105  | 5825  | 4.30       | -1.50  | 0.50  |
| HD074000  | 08 40 50.8 | -16 20 42.5 | 9.67  | 9.762 | 204  | 6166  | 4.19       | -2.02  | 0.43  |
| HD111980  | 12 53 15.1 | -18 31 20.0 | 8.38  | 8.463 | 144  | 5600  | 3.70       | -1.20  | 0.55  |
| HD160617  | 17 42 49.3 | -40 19 15.5 | 8.72  | 8.824 | 100  | 5920  | 3.60       | -1.96  | 0.46  |
| HD200654  | 21 06 34.7 | -49 57 50.3 | 9.09  | 9.215 | -48  | 5160  | 2.55       | -2.82  | 0.58  |
| HD185975  | 20 28 18.7 | -87 28 19.9 | 8.11  | 8.239 | -20  | 5780  | Solar like |        | 0.69  |
| GJ754.1A  | 19 20 34.9 | -07 40 00.0 | 12.29 | 12.38 |      | 10800 |            | DBQ5   | 0.04  |
| GD71      | 05 52 27.6 | +15 53 13.7 | 13.03 |       |      | 32300 |            | DA1    | -0.25 |
| GD153     | 12 57 02.3 | +22 01 52   | 13.34 |       |      | 38500 |            | DA1    | -0.29 |
| BD+2 3375 | 17 39 45.8 | +02 24 59   | 9.94  |       |      |       |            |        | 0.46  |





# Stellar Parameters

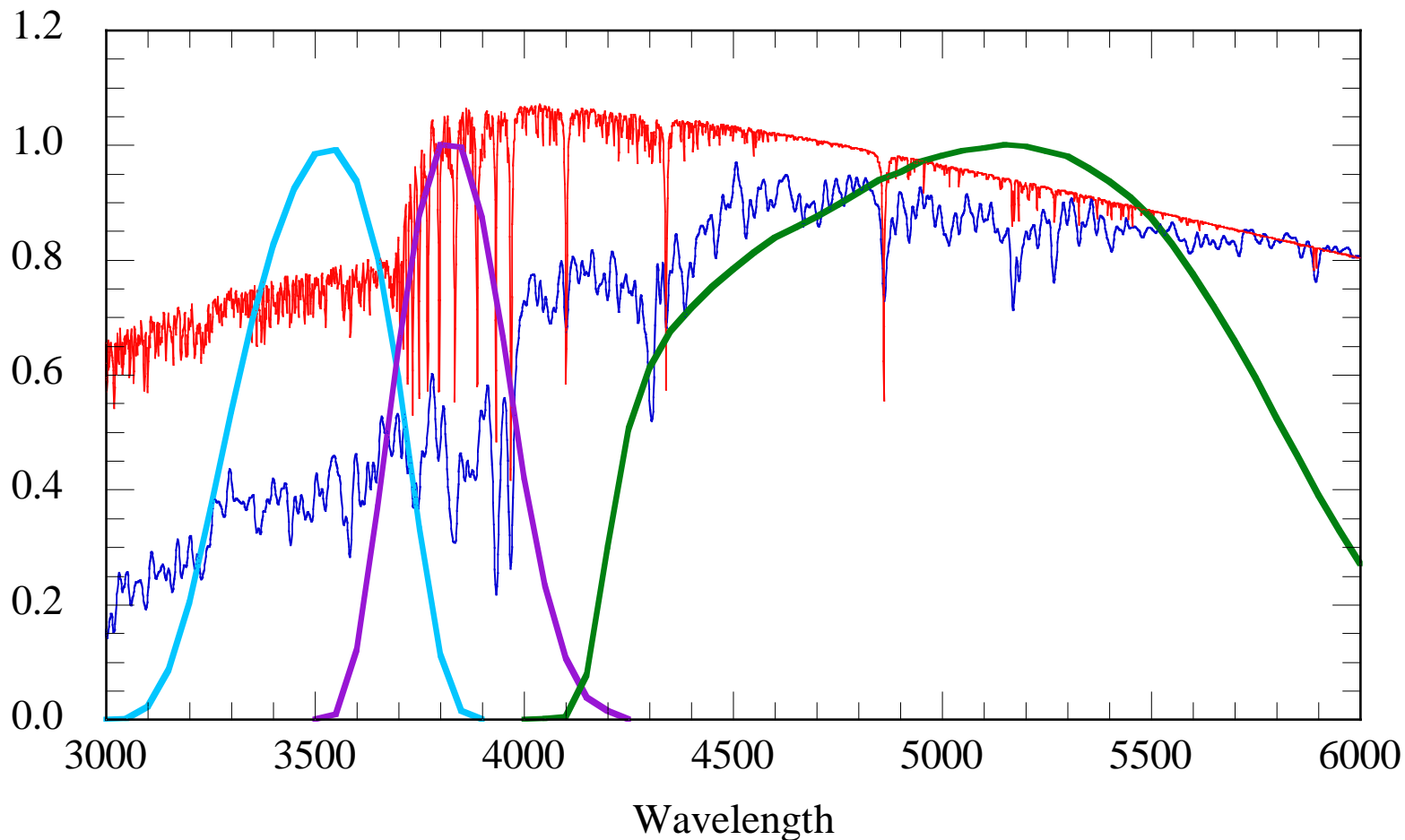
SkyMapper will determine temperature, gravity and metallicity for on the order of 100 million stars. This will be used to investigate the assembly and chemical enrichment history of the bulge, thin/thick disk and halo.

In particular, SkyMapper will isolate the most metal-poor stars for spectroscopic follow-up with AAOmega, WiFeS, FunnelWeb for eventual high resolution echelle spectroscopic analysis of the EMP (extremely metal poor) stars.

Many stars with metallicity between  $-3 > [\text{Fe}/\text{H}] > -4.5$  have already been found from follow-up spectroscopy of candidates selected from preliminary photometry of test images but the discovery of the exceptionally deficient SMSS 0313-6708 was a great surprise and boost for the SkyMapper team.



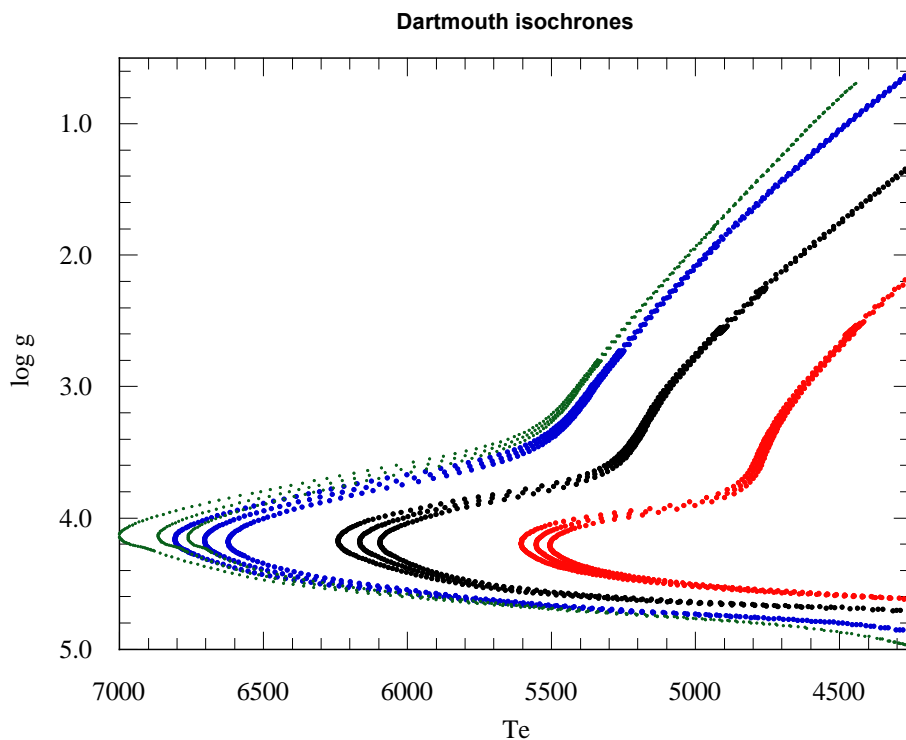
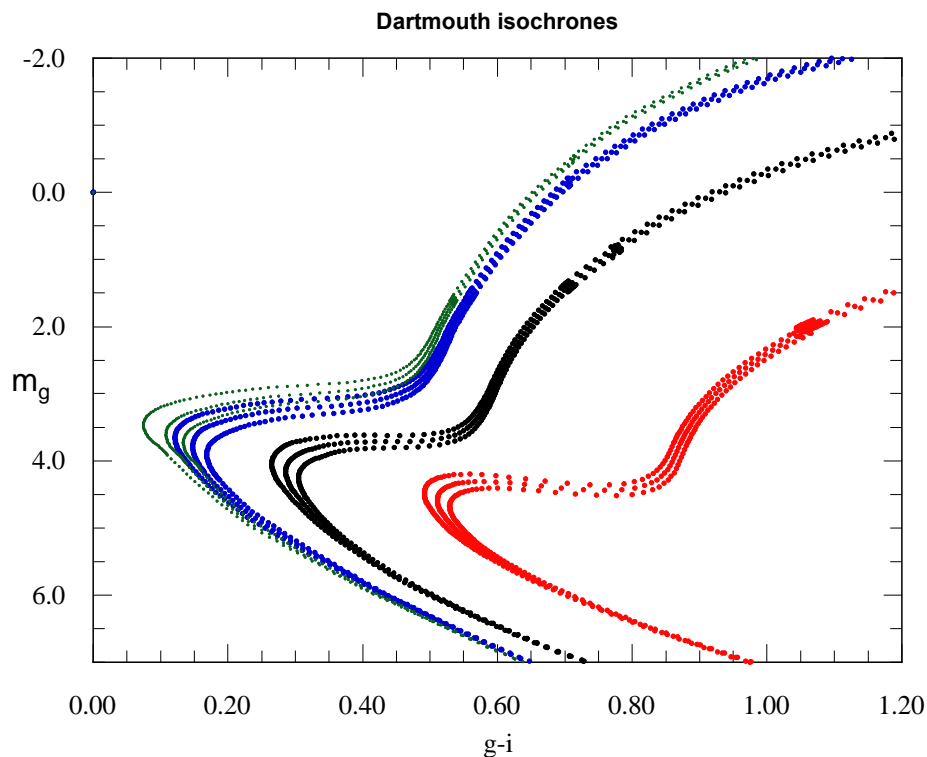
# u v g and stellar spectra



Spectra of a  $[Fe/H] = -2.5$  and  $0.0$  solar-type star with the u v g bands superimposed



# Halo isochrones



Apart from hot turnoff stars, giants are more than 10 times brighter than dwarfs at the same temperature so more likely to be observed.

Giants are easily distinguished by their much lower  $\log g$  than dwarfs.



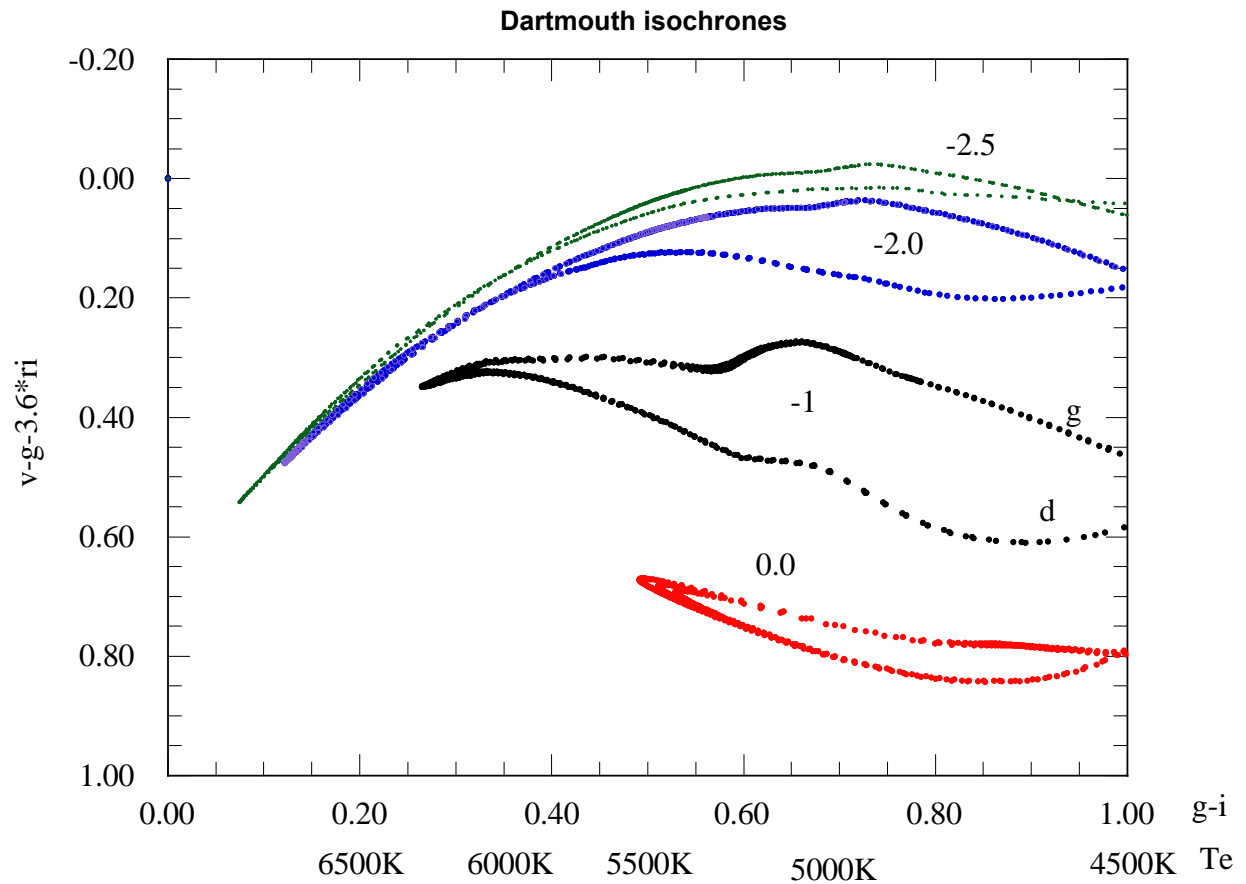


# Extremely Metal-poor Stars in the Halo

v-g is dependent on the level of the strong metal line blanketing in the violet

✓ not perturbed too much by C-enhancement

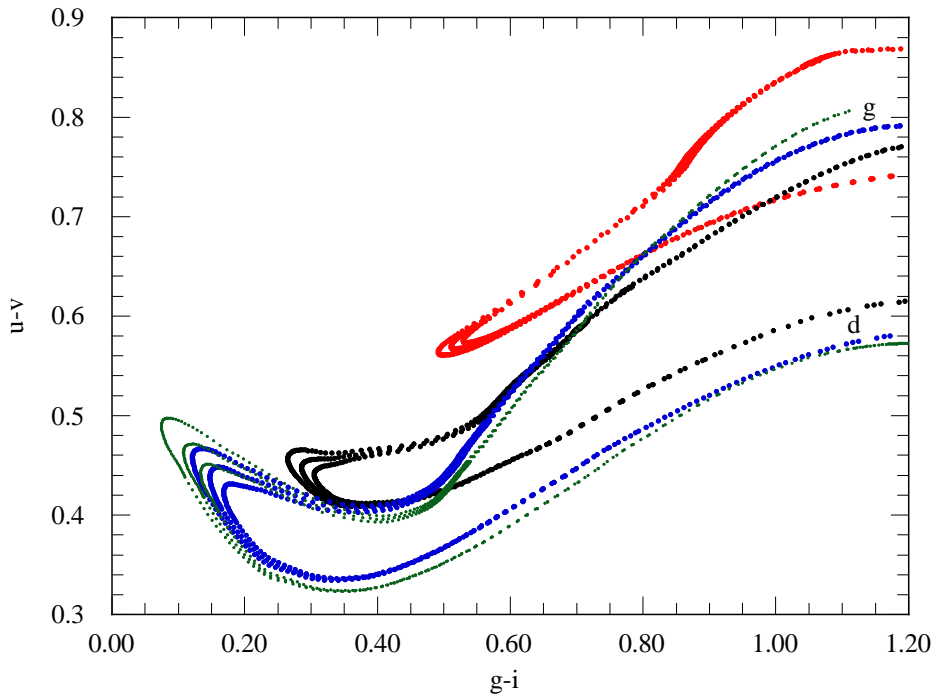
v-g retains sensitivity between -2 and -4. Should enable only stars below -3 to be followed-up spectroscopically.





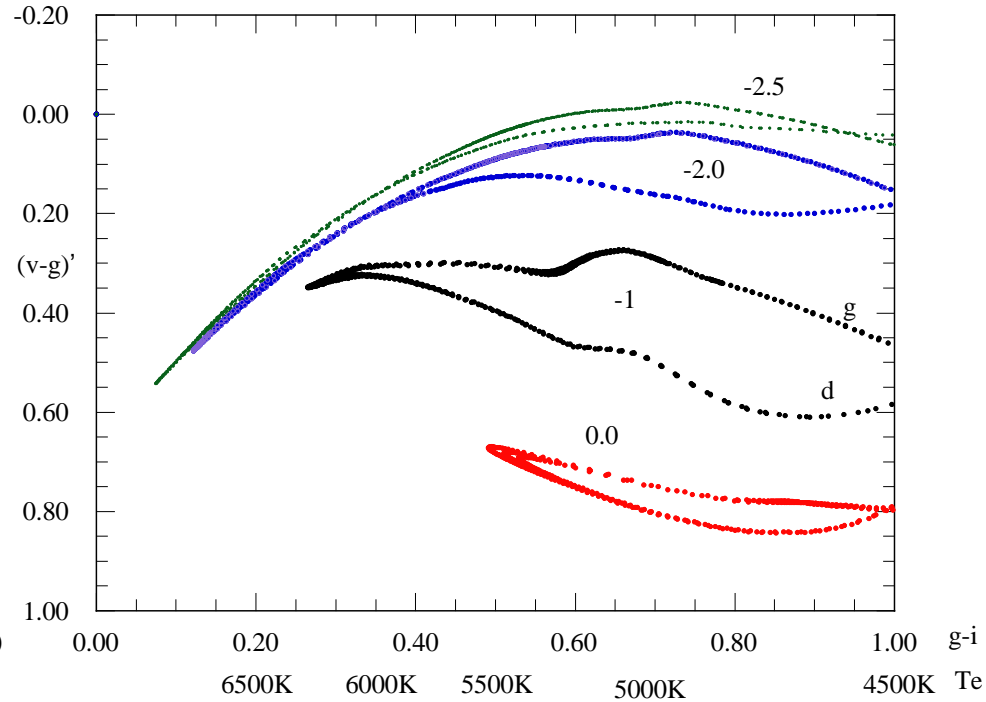
# Extremely Metal-poor Stars in the Halo

Dartmouth isochrones



Good gravity separation in  $u-v / g-i$  plane

Dartmouth isochrones

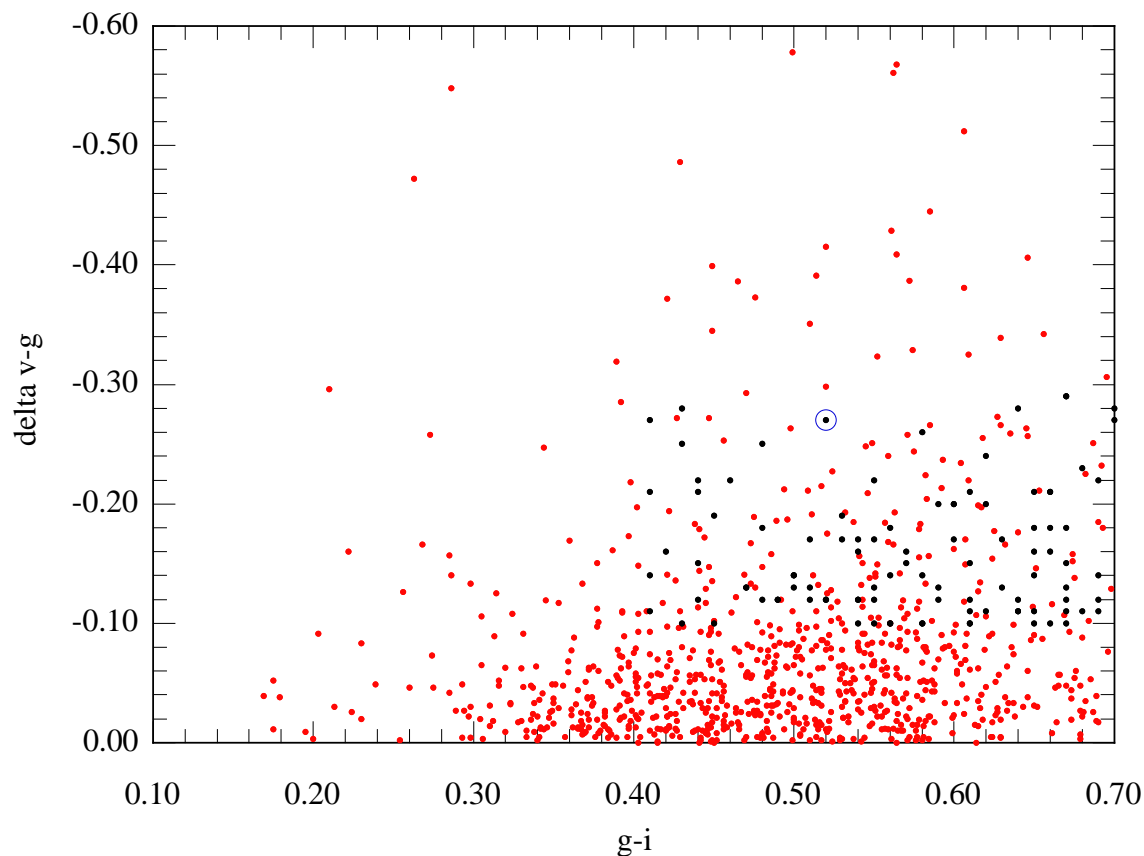


Good metallicity separation in  $v-g / g-i$  plane





# Distribution of v-g colors



The stars with the most extreme v-g excess are chosen for spectroscopic follow-up. Many of these extreme colors are errors due to the poor SkyMapper images at the time. Ca H&K emission line stars and emission line galaxies also contaminate the sample. Circled object is SMSS J0313-6708 from Jan 2013.





# WiFeS spectra of EMP stars

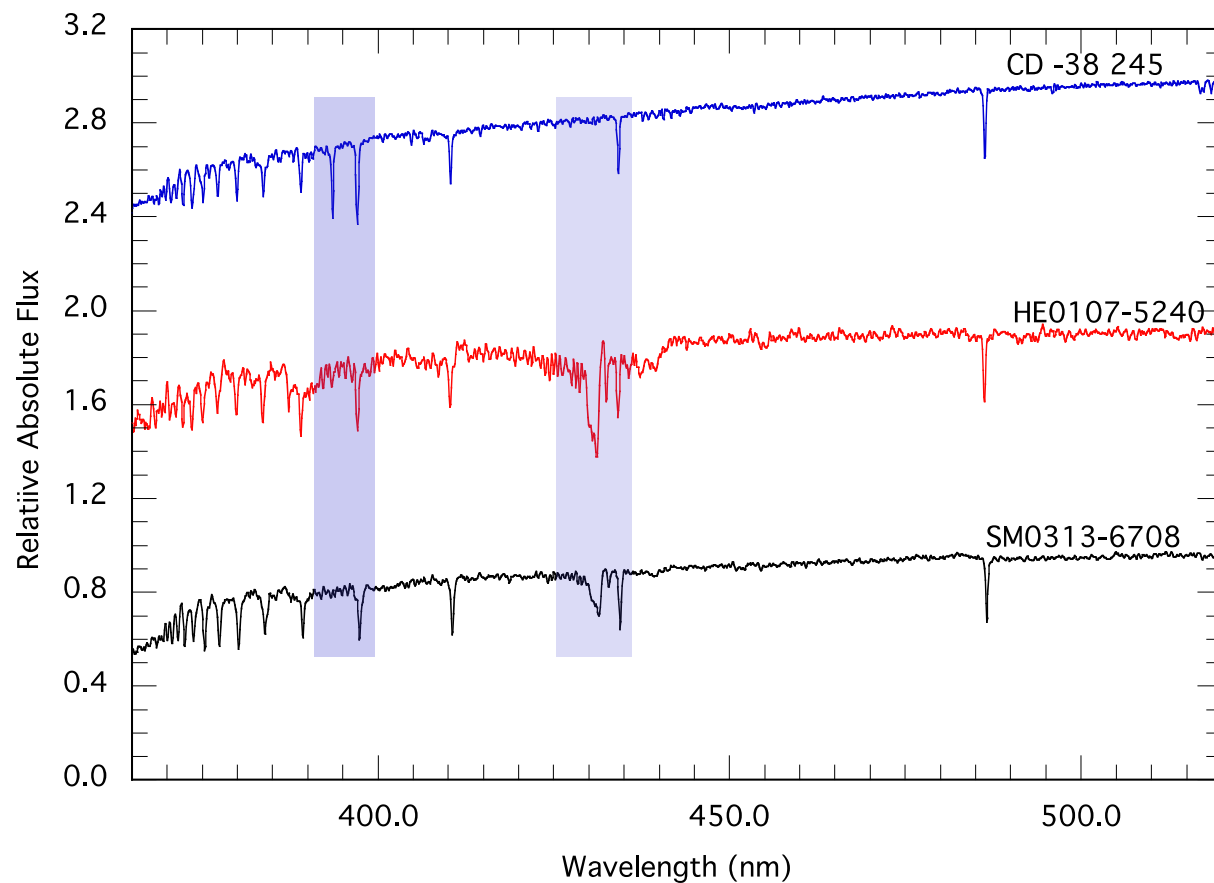
CD -38 245  $[\text{Fe}/\text{H}] = -4.1$

HE0107-5240  $[\text{Fe}/\text{H}] = -5.3$

SM0313-6708  $[\text{Fe}/\text{H}] < -7.1$

Note the region around the  
Call H&K lines and the CH  
G-band

Clearly extremely low  $[\text{Ca}/\text{H}]$   
and high  $[\text{C}/\text{H}]$  can be seen  
in WiFeS spectra.

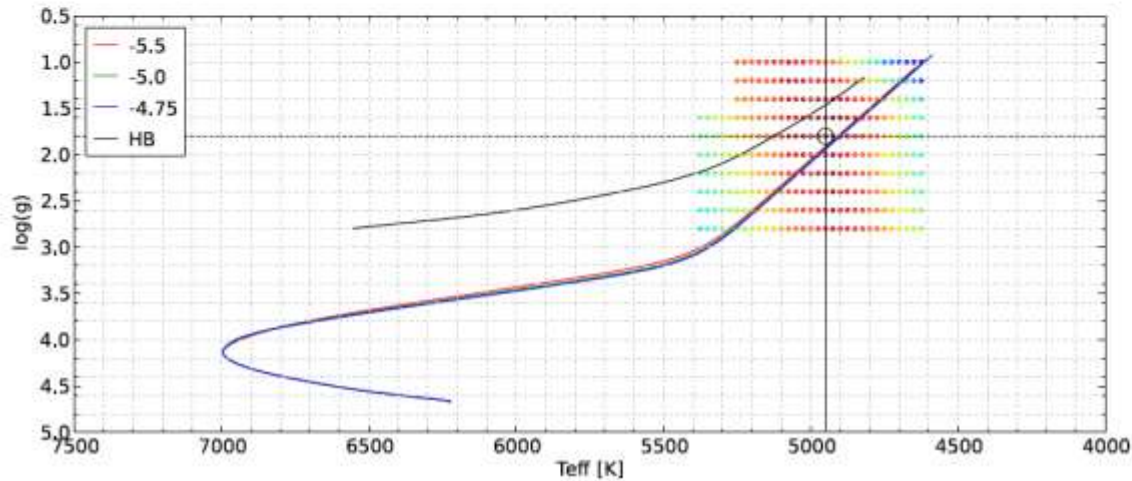
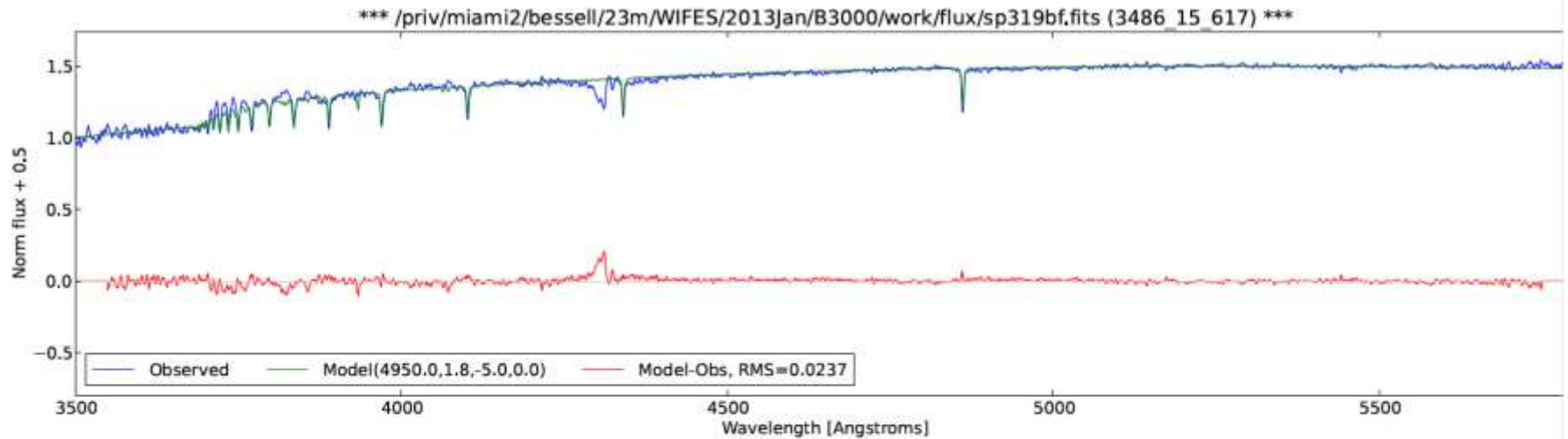


B3000 WiFeS spectra





# Fitting WiFeS spectra

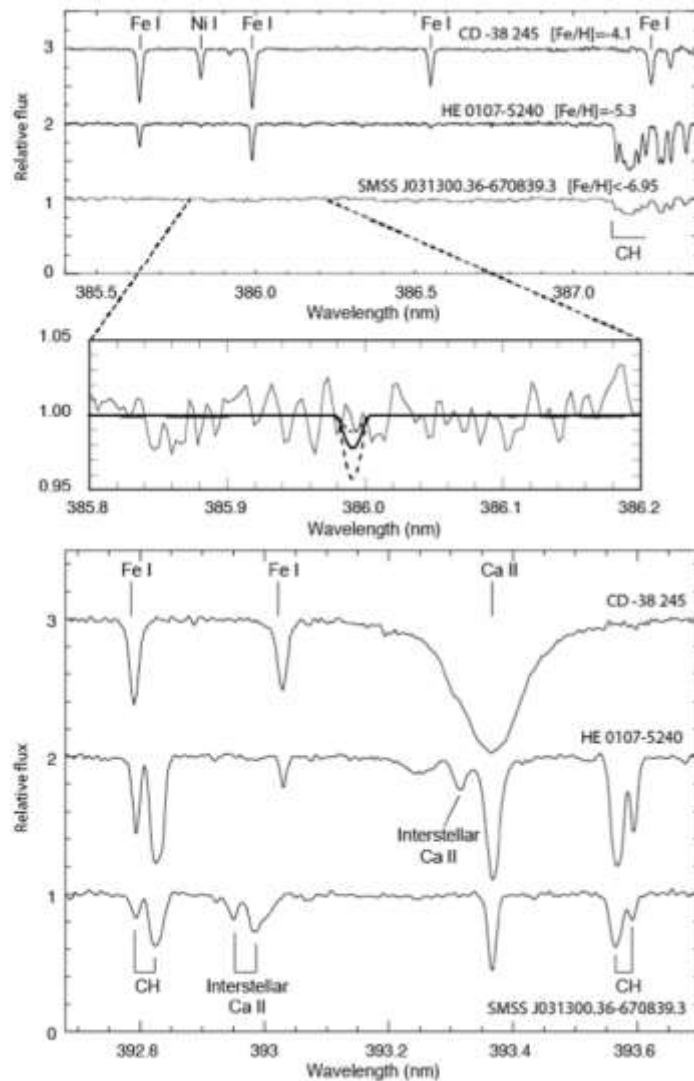
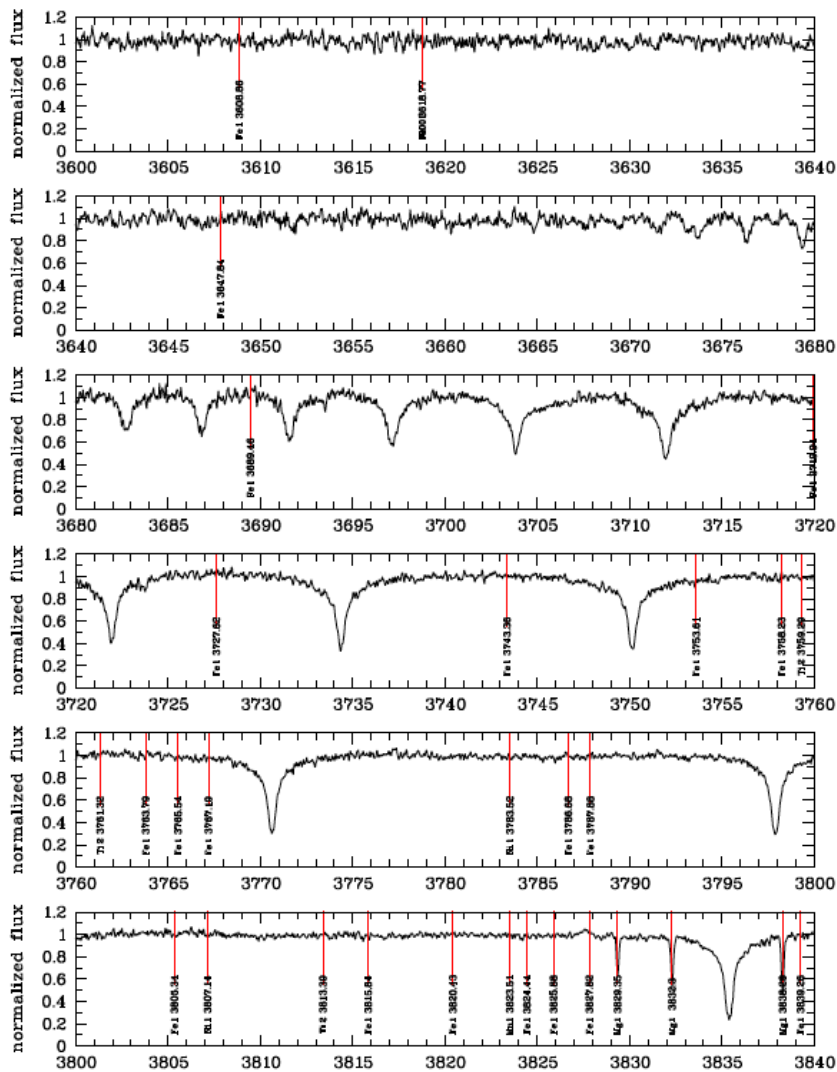


\*\*\* 3486\_15\_617 \*\*\*  
 SFD reddening: 0.037 (l,b) = (284.519,-44.587)  
 Best Model: (4950.0,1.8,-5.0)  
 Current E(B-V): 0.0  
 Radial Velocity: -342.0 km/s  
 RMS: 0.0237  
 Grid: fit\_spectra.marcs (trim=n)  
 SQL statement:  
 teff between 4000 and 7000 and logg between 0.0  
 and 5.5 and metallicity between -5.5 and 0.0





# High resolution MIKE spectrum





# Abundances and limits

**Table 1 | Chemical abundances of SMSS 0313–6708**

| Element X | $[X/H]_{1D, LTE}$ | $[X/H]_{<3D>}$ |
|-----------|-------------------|----------------|
| Li I      | 0.7*              | 0.7*           |
| C (CH)    | -2.4              | -2.6†          |
| N (NH)    | <-3.5             | <-3.9†         |
| O I       | <-2.3             | <-2.4†         |
| Na I      | <-5.5             | <-5.5‡         |
| Mg I      | -4.3              | -3.8‡          |
| Al I      | <-6.2             |                |
| Si I      | <-4.3             |                |
| Ca II     | -7.2              | -7.0‡          |
| Sc II     | <-5.0             |                |
| Ti II     | <-6.3             |                |
| V II      | <-3.3             |                |
| Cr I      | <-6.3             |                |
| Mn I      | <-5.8             |                |
| Fe I      | <-7.3             | <-7.1‡         |
| Co I      | <-4.9             |                |
| Ni I      | <-6.4             |                |
| Cu I      | <-3.5             |                |
| Zn I      | <-3.4             |                |
| Sr II     | <-6.7             |                |
| Ba II     | <-6.1             |                |
| Eu II     | <-2.9             |                |

Abundance ratios for SMSS 0313–6708 as derived from our Magellan/MIKE spectra. Typical ( $1\sigma$ ) observational uncertainties in the quoted abundances are 0.1 decades in metallicity, except in the case of C and N where 0.2 is appropriate.

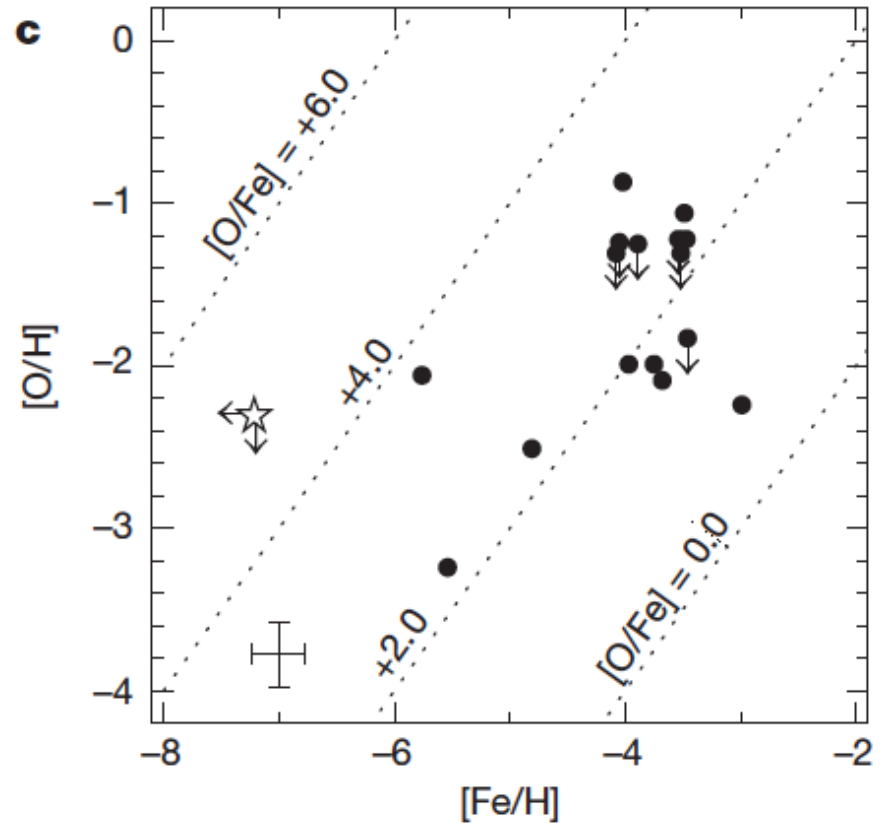
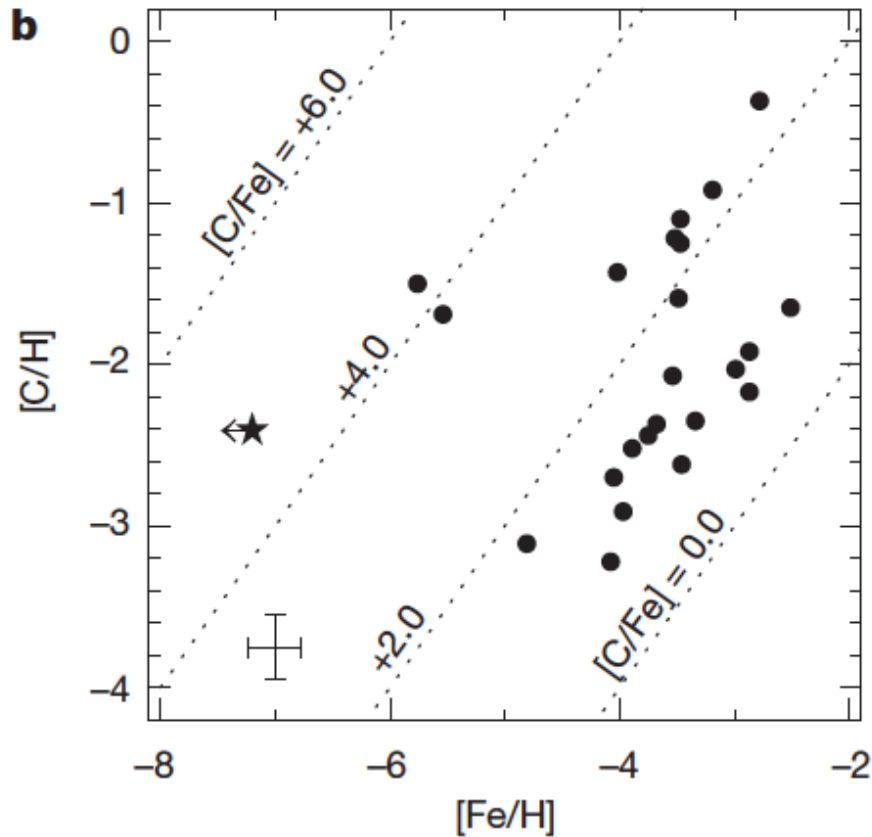
\*Lithium abundance is expressed as  $A(\text{Li}) = \log_{10}(N(\text{Li}))/N(\text{H}) + 12$ .

†Abundances based on <3D>, LTE calculations.

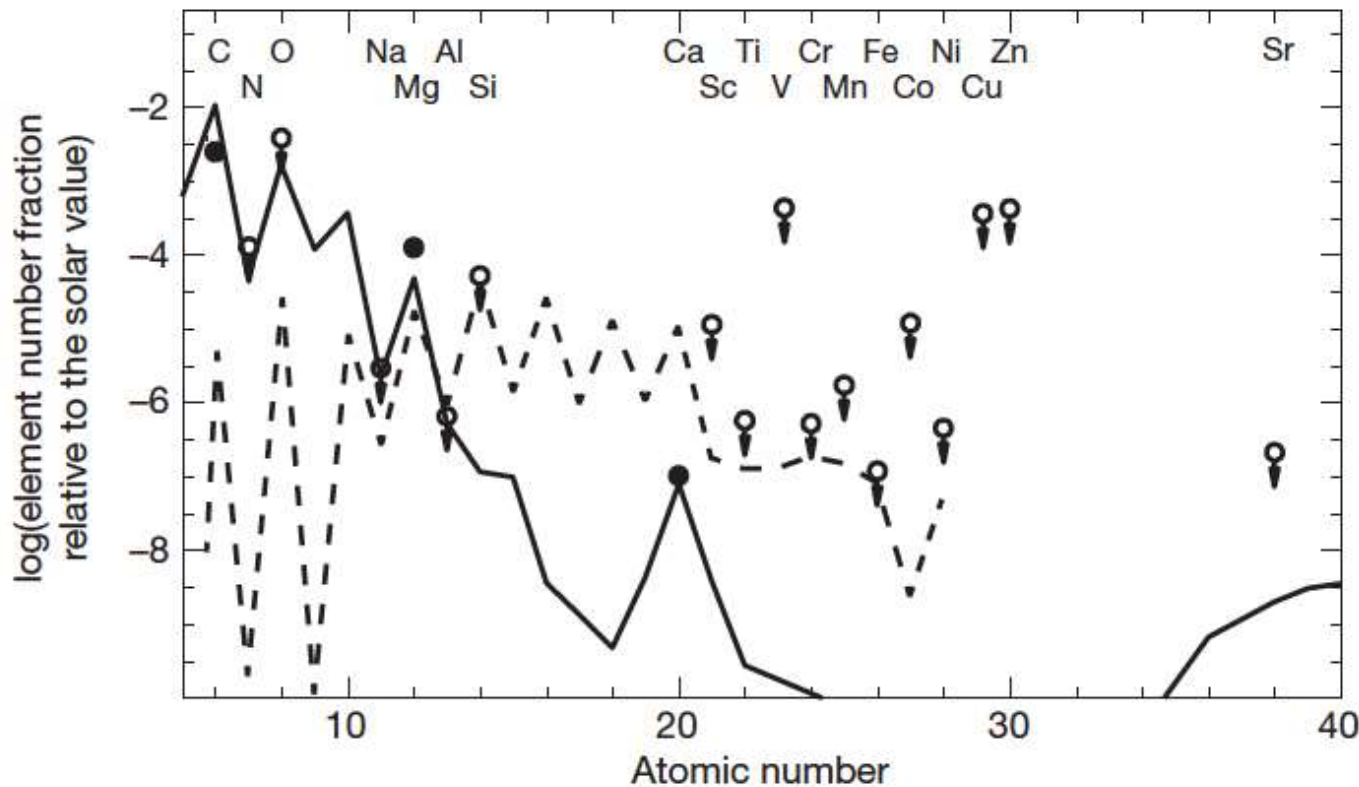
‡Abundances based on <3D>, NLTE calculations.



# Comparison with other EMP stars

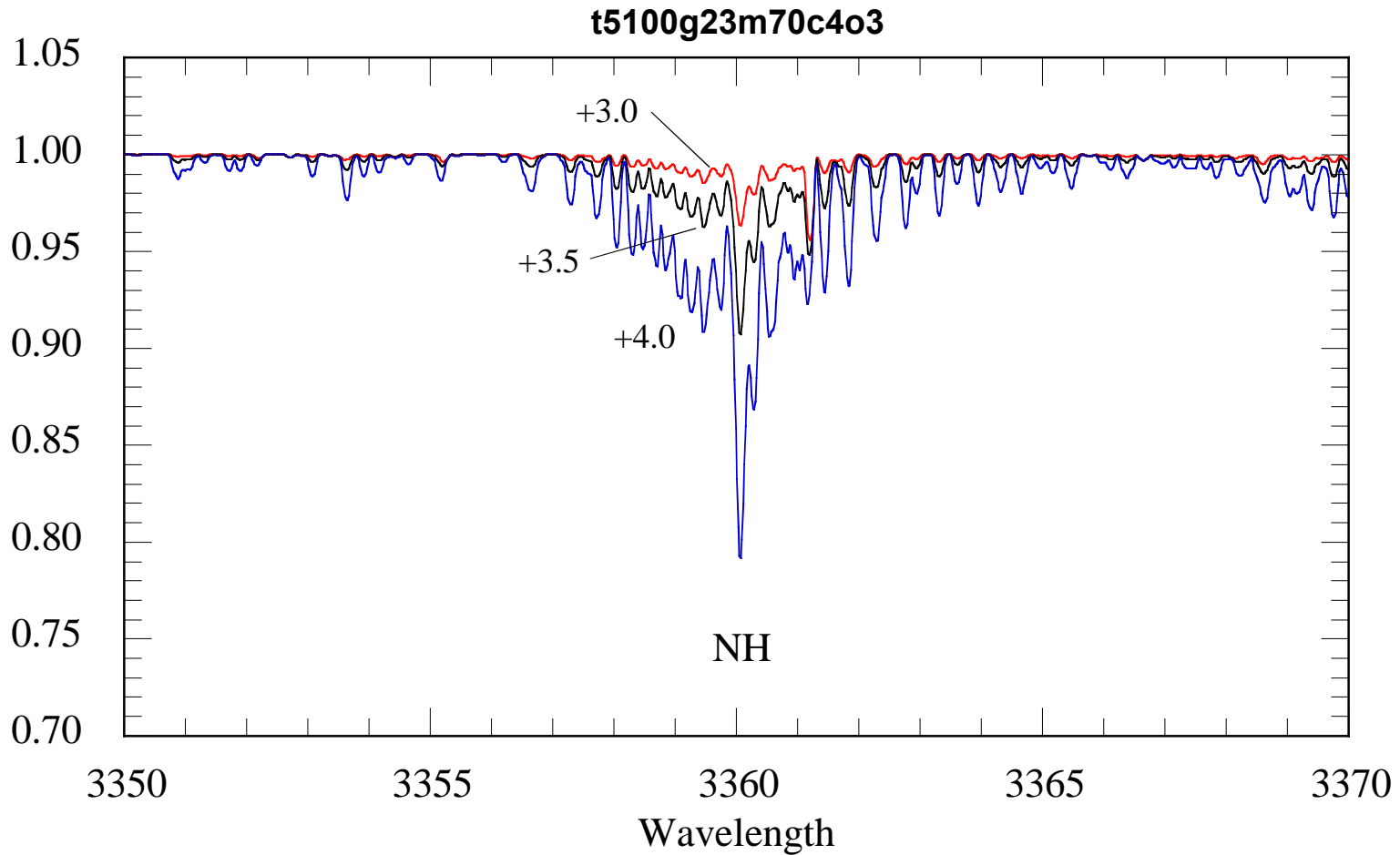


# Abundance pattern and model



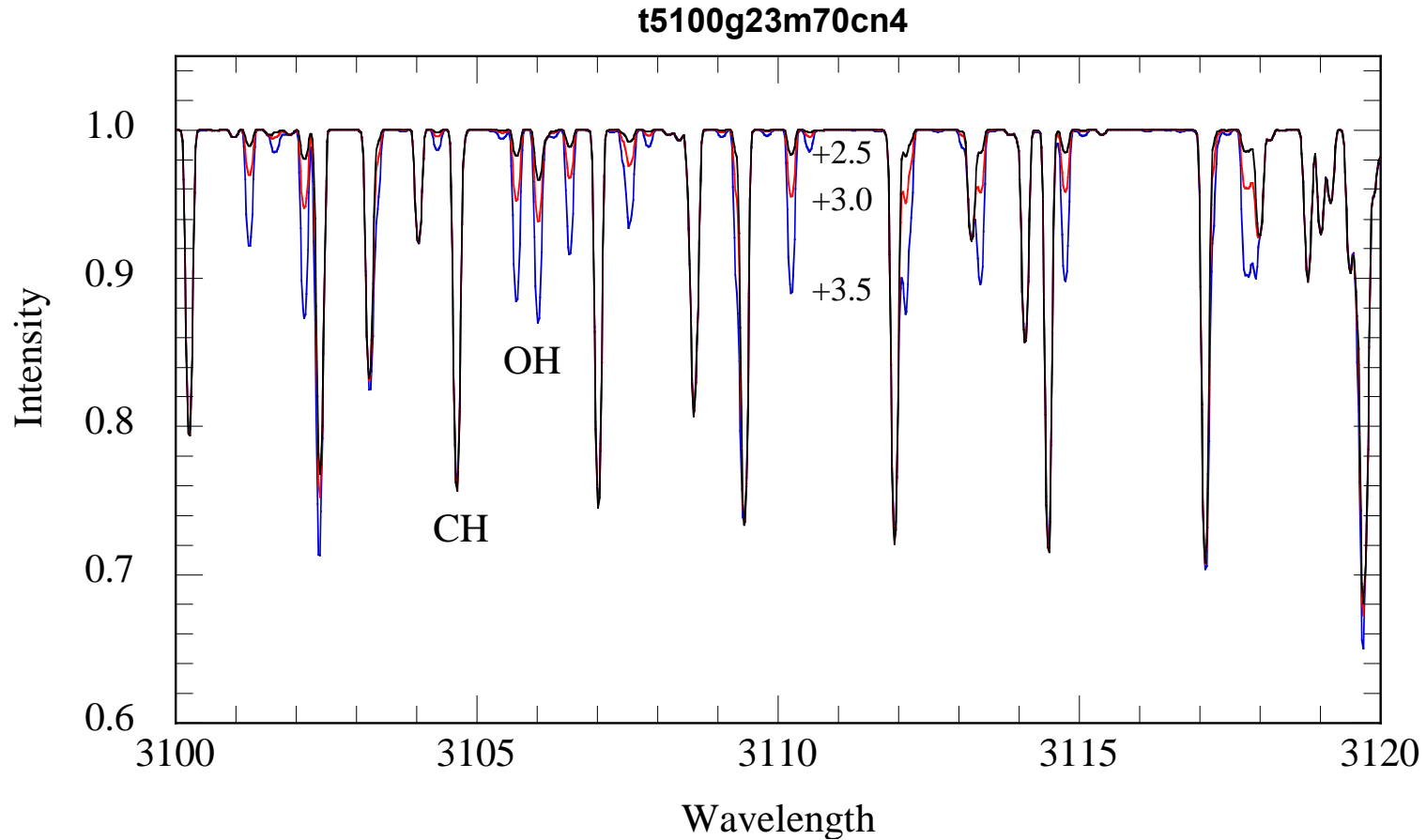
The solid line shows the abundances predicted for a  $60M_{\odot}$  population III star of relatively low explosion energy ( $1.8 \times 10^{51}$  erg) and low levels of internal mixing. The dashed line shows the expected yield from a  $200M_{\odot}$  supernova (with a pair-instability explosion mechanism). Such a massive progenitor leads to a [Mg/Ca] ratio that is much lower than that observed.

# Detection limits for nitrogen





# Detection limits for Oxygen





# Precis SMS0313-6708

- Normal Te and log g for star just above base of giant branch.
- Detection of Li I 6707A indicates that envelope/atmosphere had **normal evolution**.
- **No Fe lines seen** thus  $[\text{Fe}/\text{H}] < -7.1$ . Mg ( $[\text{Mg}/\text{H}] = -3.8$ ) and C ( $[\text{C}/\text{H}] = -2.6$ ) indicates **star formed from material seeded by SN II ejecta**.
- Galactic chemical evolution models show that stars with the iron abundance of SMSS 0313-6708 follow from a **single supernova event**.
- The observed abundance pattern does not support supernova progenitors outside the **mass range 10–70  $M_{\odot}$** .
- Ca abundance  $[\text{Ca}/\text{H}] = -7.2$  **important clue** indicating it likely formed during the hydrogen burning phase of the **60  $M_{\odot}$  primordial composition SN progenitor** star.
- The **extensive fallback of material into the black hole** traps the centrally located iron and other heavy elements synthesized during the progenitor star's lifetime.





# PRIMORDIAL STELLAR FEEDBACK AND THE ORIGIN OF HYPER-METAL-POOR STARS

TORGNY KARLSSON

NORDITA, Blegdamsvej 17, DK-2100 Copenhagen Ø, Denmark; karlsson@nordita.dk

*Received 2005 December 19; accepted 2006 February 22; published 2006 March 16*

## ABSTRACT

The apparent absence of stars in the Milky Way halo with  $-5 \leq [\text{Fe}/\text{H}] \leq -4$  suggests that the gas out of which the halo stars were born experienced a period of low or delayed star formation after the local universe was lit up by the first, metal-free generation of stars (Population III). Negative feedback due to the Population III stars could initially have prevented the pre-Galactic halo from cooling, which thereby delayed the collapse and inhibited further star formation. During this period, however, the nucleosynthesis products of the first supernovae (SNe) had time to mix with the halo gas. As a result, the initially primordial gas was already weakly enriched in heavy elements, in particular iron, at the time of formation of the Galactic halo. The very high, observed C/Fe ratios in the two recently discovered hyper-metal-poor stars HE 0107–5240 and HE 1327–2326 ( $[\text{Fe}/\text{H}] < -5$ ), as well as the diversity of C/Fe ratios in the population of extremely metal-poor stars ( $[\text{Fe}/\text{H}] < -3$ ), are then naturally explained by a combination of pre-enrichment by Population III stars and local enrichment by subsequent generations of massive, rotating stars, for which the most massive ones end their lives as black hole-forming SNe, only ejecting their outer (carbon-rich) layers. The possible existence of populations of mega-metal-poor/iron-free stars ( $[\text{Fe}/\text{H}] < -6$ ) is also discussed.





# Amazing prediction by Torgny Karlsson 2006!

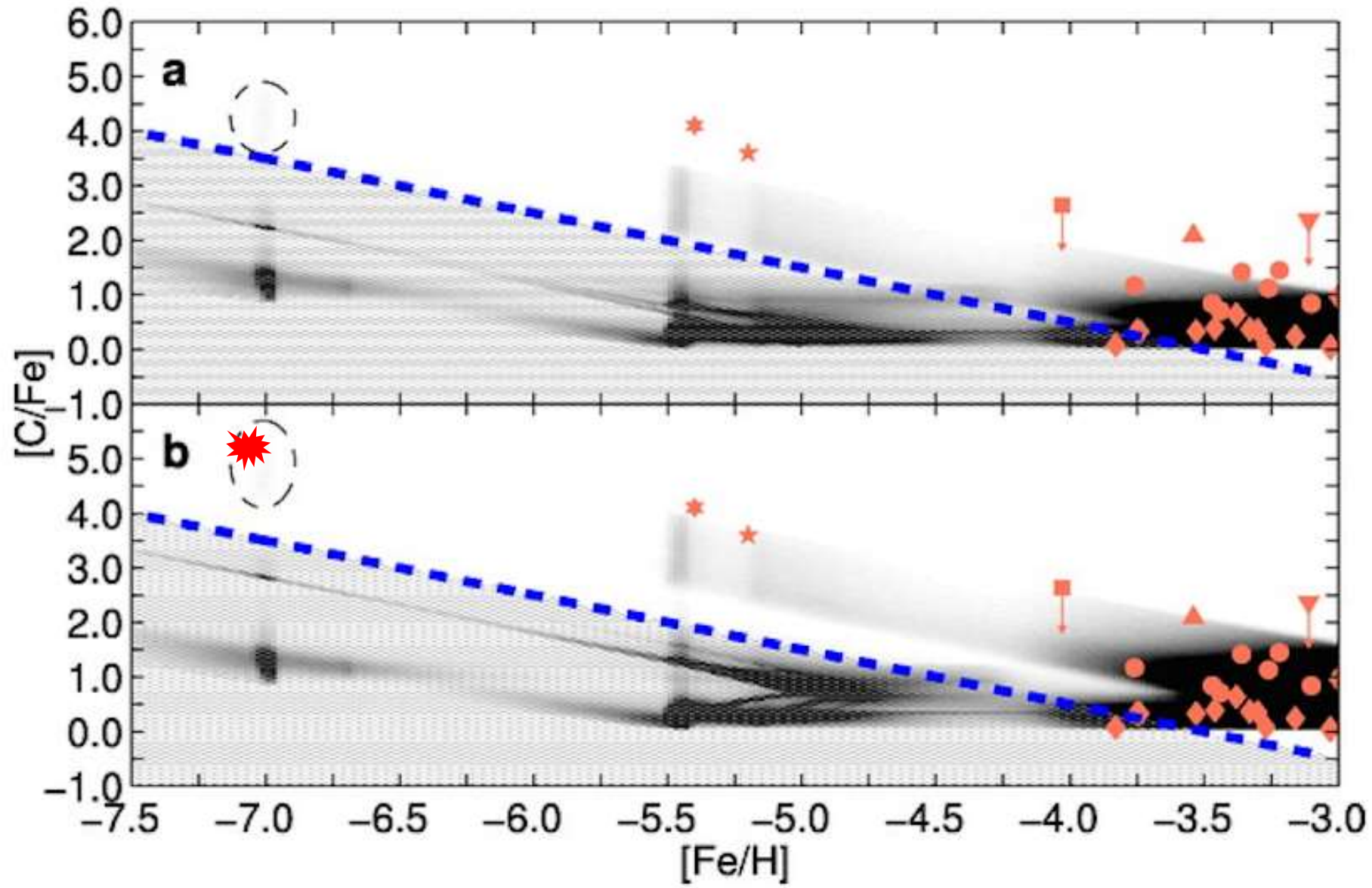




# Fig 1 Torgny Karlsson 2006

Adopted SFR in the Galactic halo (*black line*) as given by the fraction of massive stars exploding as SNe. The shaded area indicates the period of low SFR.

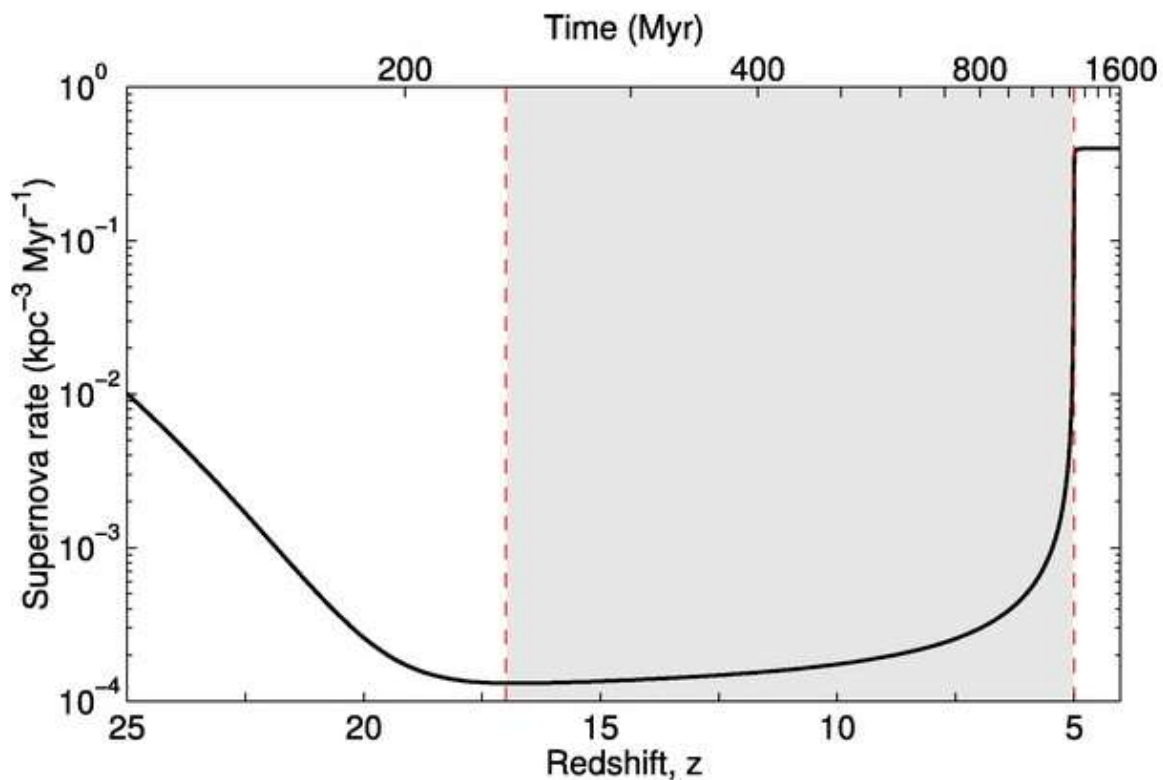
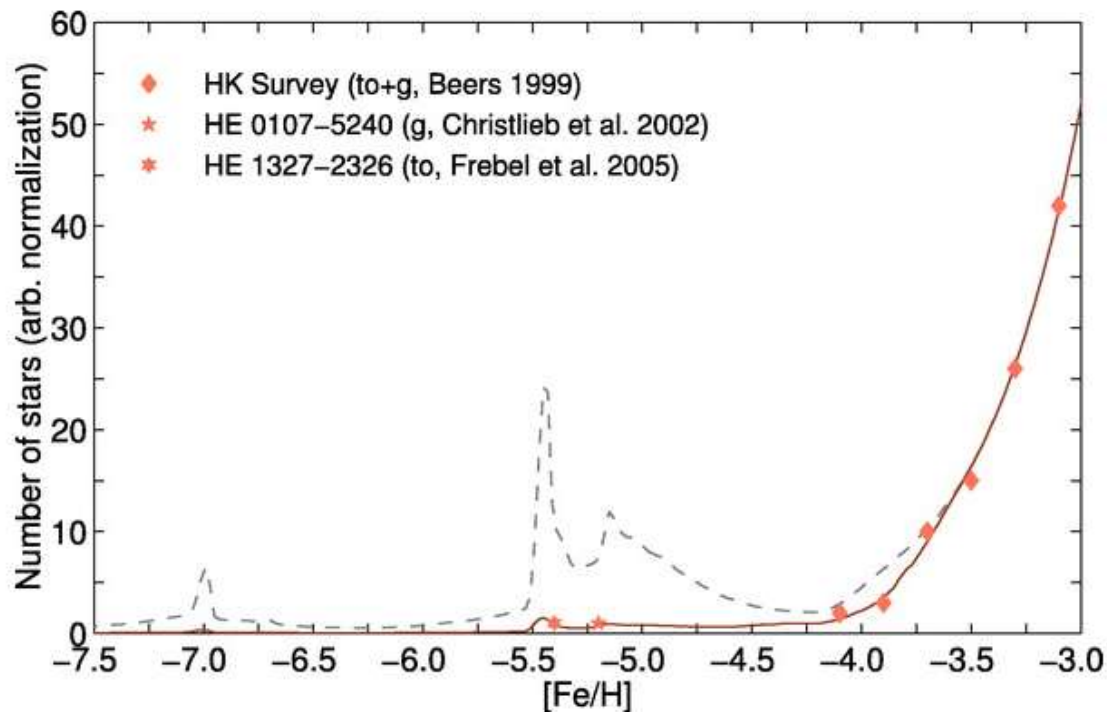




# Fig 2 Torgny Karlsson 2006

Predicted halo metallicity distribution. The dashed line denotes the distribution of stars neglecting the suppression of low-mass star formation in carbon-deficient gas. The solid line denotes the fraction of stars with carbon abundance  $[C/H] \geq -3.5$ . In both cases, a distinct population of stars appears in the range  $-5.5 \lesssim [Fe/H] \lesssim -5$ , in agreement with observations (*symbols*).





# Future work

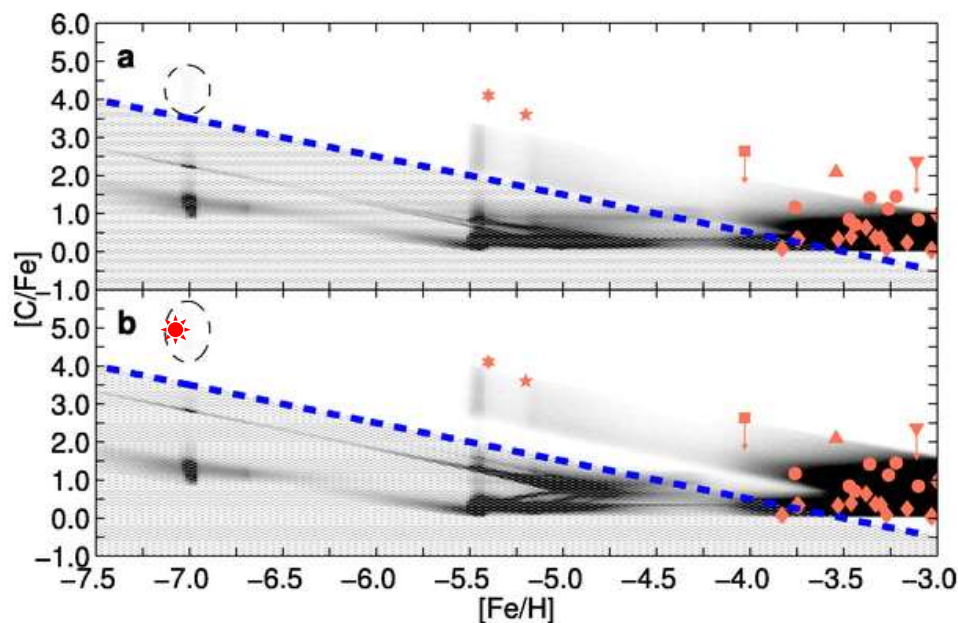
- Analyse UV VLT spectrum to get O and N abundance and UV and red spectrum to determine better limits for some metals.
- Non-LTE abundance analysis to refine results, especially for OH and NH.
- Achieve good SkyMapper photometry to increase efficiency in identifying EMP stars from WiFeS or even go directly to echelle spectroscopy.
- Compare stellar parameters  $T_e$ ,  $\log g$  and  $[Fe/H]$  determined from synthetic SkyMapper colors with those derived from spectrophotometry and fine analysis.

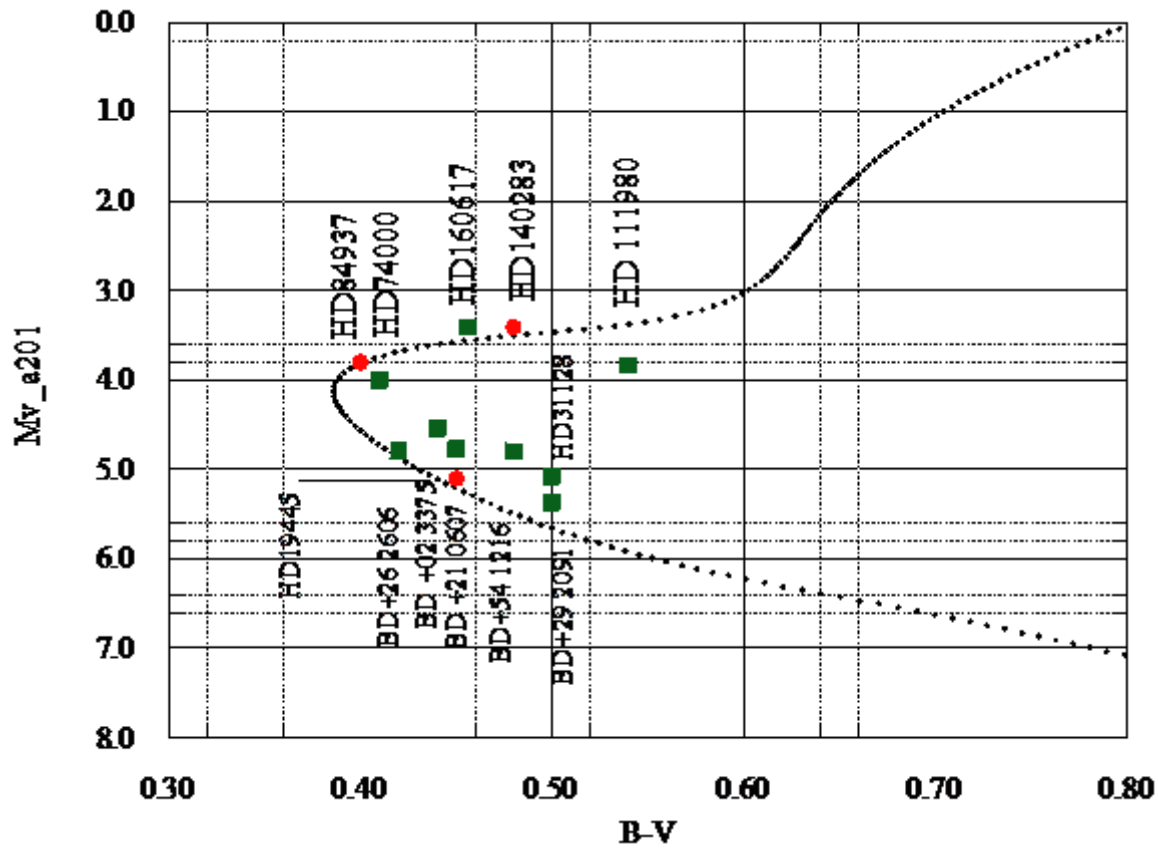




# Fig 3 Torgny Karlsson 2006

Predicted distribution of stars in the  $[C/Fe]$ - $[Fe/H]$  plane. In the top panel, the thick dashed line indicates a carbon abundance of  $[C/H] = -3.5$ . The shaded area below this limit should contain no low-mass stars (cf. Fig. 2). The symbols denote observations of stars in the Milky Way's halo. The circles are unevolved dwarf/subgiant stars (Barklem et al. 2005), the diamonds are stars on the lower red giant branch (Spite et al. 2005), the square is G77-61 (Plez & Cohen 2005), the upward facing triangle is CS 29498-43 (Aoki et al. 2004), the downward facing triangle is CS 22957-027 (Aoki et al. 2002), and, finally, the pentagon and hexagon are HE 0107-5240 (Christlieb et al. 2002) and HE 1327-2326 (Frebel et al. 2005), respectively. G77-61 and CS 22957-027 are known to be members of binary systems and may have been born with a lower surface carbon abundance as indicated by the arrows. The predicted group of mega-metal-poor stars is located inside the dashed circle. The bottom panel is the same as the upper panel, but with a carbon yield increased by a factor of 4 for stars in the mass range  $30 \leq m/M_{\odot} \leq 60$ . Note that observed abundance ratios are not corrected for three-dimensional model atmosphere effects.







# Blue Horizontal Branch Stars

